

1 Allelic variants of the NLR protein Rpi-chc1 differentially  
2 recognise members of the *Phytophthora infestans*  
3 PexRD12/31 effector superfamily through the leucine-  
4 rich repeat domain

5  
6 Daniel Monino-Lopez <sup>1</sup>, Maarten Nijenhuis <sup>1,2</sup>, Linda Kodde <sup>1</sup>, Sophien Kamoun <sup>3</sup>, Hamed  
7 Salehian <sup>1</sup>, Kyrylo Schentsnyi <sup>1,5</sup>, Remco Stam <sup>1,6</sup>, Anoma Lokossou <sup>1</sup>, Ahmed Abd-El-Haliem  
8 <sup>1,8</sup>, Richard GF Visser <sup>1</sup>, Jack H Vossen <sup>1\*</sup>

9  
10 <sup>1</sup> Plant Breeding, Wageningen University & Research, Droevendaalsesteeg 1, 6708PB,  
11 Wageningen, The Netherlands.

12 <sup>2</sup> Current address: Agrico Research, Burchtweg 17, 8314PP, Bant, The Netherlands;

13 <sup>3</sup> The Sainsbury Laboratory, University of East Anglia, Norwich Research Park, Norwich,  
14 United Kingdom.

15 <sup>5</sup> Current address: Center for Plant Molecular Biology, Auf der Morgenstelle 32, 2076  
16 Tübingen, Germany;

17 <sup>6</sup> Current address: Technical University Munich;

18 <sup>8</sup> Current address: Rijk Zwaan Breeding B.V., Burgemeester Crezéelaan 40, The  
19 Netherlands;

20

21 \* Corresponding author:

22 Jack H. Vossen

23 +31 317 481 590

24 [jack.vossen@wur.nl](mailto:jack.vossen@wur.nl)

25

26

27 Word count: Total: 6,301 words; Summary: 200 words; Introduction: 854 words; Materials

28

and Methods: 1,284 words; Results: 2,543 words; Discussion: 1,612 words.

29

30

Number of figures: 6 (all in colour)

31

Number of Tables: 0

32

Number of supplementary Figures: 5 (all in colour)

33

Number of supplementary Tables: 7

## 34 **Summary**

- 35 • *Phytophthora infestans* is a pathogenic oomycete that causes the infamous  
36 potato late blight disease. Resistance (*R*) genes from diverse *Solanum* species  
37 encode intracellular receptors that recognize *P. infestans* RXLR effector proteins  
38 and provide effective defence responses. To deploy these *R* genes in a durable  
39 fashion in agriculture, we need to understand the mechanism of effector  
40 recognition and the way the pathogen evades recognition.
- 41 • We cloned sixteen allelic variants of the *Rpi-chc1* gene from *Solanum chacoense*  
42 and other *Solanum* species, and identified the cognate *P. infestans* RXLR  
43 effectors. These tools were used to study receptor-ligand interactions and co-  
44 evolution.
- 45 • Functional and non-functional alleles of *Rpi-chc1* encode Coiled-Coil–Nucleotide  
46 Binding–Leucine-Rich-Repeat (CNL) proteins. *Rpi-chc1.1* recognised multiple  
47 PexRD12 (AVRchc1.1) proteins while *Rpi-chc1.2* recognised multiple PexRD31  
48 (AVRchc1.2) proteins, both from the PexRD12/31 superfamily. Domain swaps  
49 between *Rpi-chc1.1* and *Rpi-chc1.2* revealed that overlapping subdomains in the  
50 LRR were responsible for the difference in effector recognition.
- 51 • This study showed that *Rpi-chc1.1* and *Rpi-chc1.2*, evolved to recognize distinct  
52 members of the same PexRD12/31 effector family via the LRR domain. The  
53 biased distribution of polymorphisms suggests that exchange of LRRs during  
54 host-pathogen co-evolution can lead to novel recognition specificities. These  
55 insights will help future strategies to breed for durable resistant varieties.

56 **Key words:** NLR cluster, Leucine rich repeat *Phytophthora infestans*, Late blight  
57 resistance gene, RXLR effector, *Solanum* species, potato

58

59

60

61

62

63

64

65

## 66 **Introduction**

67 Potato (*Solanum tuberosum*) is the fourth largest food crop in the world after maize,  
68 rice and wheat, with more than 368 million tonnes produced in 2018 (FAO, 2020).  
69 Potato late blight, caused by the oomycete *Phytophthora infestans* (*P. infestans*), is  
70 one of the most infamous potato diseases. During the mid-1840s, this pathogen  
71 caused the Great Irish Famine from which around one million people died (Callaway,  
72 2013). Nowadays, losses from late blight are estimated to still reach 16% of the world  
73 production and the main disease management is based on biocide applications.  
74 Including yield losses and crop protection measures, late blight causes a global  
75 economic loss of € 5.2 billion per year (Haverkort *et al.*, 2016).

76  
77 *P. infestans* is an oomycete with sexual and asexual life cycles, which exhibits a  
78 hemibiotrophic lifestyle on potato. Together with its large and fast evolving genome, it  
79 leads to the regular emergence of new aggressive and virulent strains. The infection  
80 starts when a spore lands on the plant surface, germinates and forms a penetration  
81 structure called appressorium. Alternatively, spores can also enter through natural  
82 openings such as stomata. After passing the epidermis, hyphae spread intercellularly  
83 projecting haustorium structures into the mesophyll cells. These haustoria are  
84 specialised infection structures that create an intimate association with the host cell  
85 facilitating nutrient uptake, and both apoplastic and cytoplasmic effector secretion  
86 (Fry, 2008). Effectors are pathogen molecules that interact with different host targets  
87 to suppress the host defence response and enable colonisation. The publication of  
88 the *P. infestans* T30-4 genome, revealed the presence of 563 effector genes  
89 encoding the conserved Arg-any amino acid-Leu-Arg (RXLR) peptide motif (Haas *et al.*,  
90 2009). These effectors, rapidly evolve by gaining and losing repeat-rich domains  
91 through recombination with different paralogs, transposon movement, and point  
92 mutations (Goss *et al.*, 2013). During co-evolution, potato has evolved receptors to  
93 recognise some of these effectors and trigger an immune response.

94  
95 Wild *Solanum* species are the main source of resistance (*R*) genes to *P. infestans*  
96 (*Rpi*). To date, over 20 *Rpi* genes have been characterised in different *Solanum*  
97 species, e.g. *R1*, *R2*, *R3a*, *R3b*, *R8*, *R9a* from *S. demissum*, *Rpi-blb1*, 2 from *S.*  
98 *bulbocastanum*, *Rpi-vnt1* from *S. venturii* and *Rpi-amr1* from *S. americanum*

99 (Ballvora *et al.*, 2002; van der Vossen *et al.*, 2003, 2005; Huang *et al.*, 2005; Pel *et*  
100 *al.*, 2009; Lokossou *et al.*, 2009; Li *et al.*, 2011; Jo *et al.*, 2015; Vossen *et al.*, 2016;  
101 Witek *et al.*, 2020). All these receptors belong to the nucleotide-binding (NB)–leucine-  
102 rich repeat (NLR) type of receptors and contain a coiled-coil domain (CC) in their N-  
103 termini, referred to as CC-NB-LRR or CNL. The recognition of a specific effector or a-  
104 virulence factor (AVR) leads to the activation of the plant defences and the restriction  
105 of the pathogen growth. To keep up with the fast evolution of effectors, NLR genes  
106 are also very diverse and rapidly evolving. Gene duplications, recombinations,  
107 unequal crossing overs and transpositions have been proposed to provide the basis  
108 for the evolution of the NLR recognition spectrum (Leister, 2004; Mcdowell & Simon,  
109 2006). This fast evolution can lead to the independent development of new Rpi  
110 receptors in different geographical locations that recognise the same effector. For  
111 instance, the recognition of the effector AVR2 from *P. infestans*, by the unrelated R2  
112 and Rpi-mcq1 CNLs (Aguilera-Galvez *et al.*, 2018). R2 is located on chromosome IV  
113 in the Mexican species *S. demissum*, while Rpi-mcq1 is located on chromosome IX  
114 from a Peruvian accession of *S. mochiense* (Smilde *et al.*, 2005; Foster *et al.*,  
115 2009). When the doubled-monoploid DM1-3 519 R44 potato genome was published,  
116 755 NLR genes were identified (Jupe *et al.*, 2013). Many of them were found in  
117 clusters together with closely related paralogs. All of these clusters were formed in  
118 ancestral species and had sequence homology to syntenic genomic regions from  
119 other *Solanum* species harbouring late blight resistance genes. Thus, inactive *Rpi*  
120 homologs (*rpi*) can be found in all *Solanum* genomes.

121

122 Here, we studied *Solanum chacoense* (*S. chacoense*); a diploid wild potato relative  
123 from South America considered a source of resistance to *P. infestans*. We identified  
124 two functionally distinct receptors, Rpi-chc1.1 and Rpi-chc1.2, which are allelic  
125 variants that recognise distinct *P. infestans* effectors from the same PexRD12/31  
126 effector superfamily. Remarkably, only Rpi-chc1.1 is able to provide resistance  
127 against current *P. infestans* isolates. The expression and recognition of PexRD12  
128 effectors was associated with Rpi-chc1.1 mediated resistance and, therefore,  
129 designated as AVRchc1.1 effectors. PexRD31 effectors were still expressed in  
130 current *P. infestans* isolates, but were rapidly downregulated during the interaction  
131 with potato. This, potentially explains the inability of *Rpi-chc1.2* to provide late blight  
132 resistance. We postulate that *Rpi-chc1.2* is a ubiquitous ancient *R* gene that was

133 recently overcome and PexRD31 may have functioned as AVRchc1.2. An allele  
134 mining strategy revealed Rpi-chc1 orthologs in different wild *Solanum* accessions  
135 and potato cultivars that could be classified by their sequence and recognition  
136 spectrum of AVRchc1.1, AVRchc1.2, or non-functionality. Finally, using domain  
137 swaps, we found that the LRR domain harboured the recognition specificity of both  
138 AVRchc1.1 and AVRchc1.2. The specificities resided in overlapping LRR  
139 subdomains and could not be combined into one active protein using domain  
140 exchanges.

## 141 **Materials and Methods**

142

### 143 **Plant materials and growth conditions**

144 The wild *Solanum* species used in this study are listed in **Table S1** (Tan *et al.*, 2010;  
145 Vleeshouwers *et al.*, 2011a). The potato plants were maintained *in vitro* on MS20 at  
146 24°C under 16/8h day/night regime (Domazakis *et al.*, 2017). The 7650 F1 population  
147 was generated by crossing *S. chacoense* (CHC543-5) x *S. chacoense* (CHC544-5).  
148 *S. tuberosum* cv. 'Desirée' was used for stable transformations of the different *Rpi-*  
149 *chc1.1* candidates. Four week old *Nicotiana benthamiana* leaves were used for  
150 agroinfiltration. The agroinfiltrated plants were kept in climate regulated greenhouse  
151 compartments of Unifarm (Wageningen University & Research) at 20-25°C and under  
152 16/8h day/night regime.

153

### 154 **BAC clone isolation and sequencing**

155

156 The procedure has been described in patent US9551007B2. Briefly: Two different  
157 BAC libraries were produced using partial digestion of CHC543-5 genomic DNA with  
158 HindIII. Fragments larger than 100kb were ligated into pBeloBAC or pCC1BAC arms  
159 (Epicenter). The BAC clones were collected and stored as bacterial pools of  
160 approximately 700 to 1000 white colonies. BAC pools were screened with selected  
161 markers and individual clones were identified using colony PCR. The ends of positive  
162 individual BACs were sequenced for the purpose of fine mapping RH106G03T and  
163 RH137D14\_C37-7-4. The complete inserts were sequenced using shotgun  
164 sequencing of 2kb library fragments generated by partial digestion with EcoR1 by

165 Macrogen, Inc (Seoul, South Korea). Assembly of the sequences resulted in contigs  
166 as indicated in Fig. 1 (Genbank accession number MW383255).

167

### 168 **Cloning of *Rpi-chc1* allelic variants and chimeric constructs**

169

170 The *Rpi-chc1* allelic variants were amplified using genomic DNA from the different  
171 wild *Solanum* species using PCR primers as described in Table **S2** and DNA  
172 polymerase with proofreading activity. The fragments were cloned into pGEM-T easy  
173 vector (Promega) for sequencing. Genbank submission numbers as in Table **S1**. The  
174 *Rpi-ber1.1* and *Rpi-tar1.1* genes were amplified using primers in the promotor and  
175 terminator. The resulting PCR fragments were cloned into pBINPLUS-PASSA (Jo *et*  
176 *al.*, 2016) and were expressed in transgenic Desiree plants under the control of their  
177 native regulatory elements. For transient expression analyses, the coding sequences  
178 of the allelic variants were cloned under the *Rpi-chc1.1* regulatory elements (900bp  
179 promotor and 400bp terminator) into pDEST using a multisite gateway protocol.  
180 *Escherichia coli* strain DH10 $\beta$  was transformed with the gateway reaction products  
181 and clones with the correct insert were selected. *Agrobacterium tumefaciens*  
182 AGL1+VirG was used for transient and stable transformations of *N. benthamiana*  
183 leaves and *S. tuberosum* cv. 'Désirée' .

184

185 The chimeric constructs were cloned using the Golden Gate modular cloning  
186 principle. As acceptor vector, we used a Golden Gate compatible version of  
187 pBINPLUS (McBride & Summerfelt, 1990), PBINPLUS-GG (Vossenber *et al.*, 2019).  
188 The final acceptor vector was constructed to contain 800bp *Rpi-chc1.1*  
189 promoter::CDS::1000bp *Rpi-ber* terminator (Fig. **S1**). The different PCR fragments  
190 were amplified using the Phusion High-Fidelity PCR Kit (Thermo SCIENTIFIC) and  
191 primers with Bsal sites as overhang (Table **S2**) and purified using the DNA  
192 Clean&Concentrator Kit (ZYMO RESEARCH). PCR fragments and the acceptor  
193 vector were incubated in Buffer G (Thermo SCIENTIFIC) with ATP 1mM for thirty  
194 cycles of 37°C for 5min + 16°C for 5min. Additionally, we performed a final step at  
195 37° for 10min, to digest the plasmids wrongly assembled, and 65°C for 20min, to heat  
196 inactivate the Bsal enzyme.

197

### 198 **Hypersensitive cell death assays**

199

200 Transient expression of the different receptors and PexRD12/31 effectors were  
201 performed in four weeks old *N. benthamiana* leaves. R3a/AVR3a was used as a  
202 positive control. All the constructs were agroinfiltrated at an OD<sub>600</sub> of 0.5. Each  
203 construct was agroinfiltrated twice on two leaves of four plants in at least two  
204 independent experiments. Cell death responses were observed after 3-4 days post  
205 inoculation.

206

### 207 **Phylogenetic analysis of Rpi-chc1.1 homologs and the PexRD12/31** 208 **superfamily**

209

210 The sequences of the PexRD12/31 effectors were retrieved from the *P. infestans*  
211 T30-4 genome (Haas *et al.*, 2009). Twenty family members were found to form the  
212 PexRD12/31 superfamily. The coding sequences of the *Rpi-chc1* variants as  
213 obtained in this study, were aligned using MUSCLE and a neighbour joining tree was  
214 calculated using Megalign from the DNASTAR package. The closest homolog of *Rpi-*  
215 *chc1.1* from the DM reference genome (SoltuDM10G021850.1) was used as an  
216 outgroup.

217 The protein sequences of PexRD12/31 effectors were aligned using Clustal OMEGA  
218 and manually edited in MEGAX (Sievers *et al.*, 2011; Kumar *et al.*, 2018). The  
219 phylogenetic relationship was inferred using the Maximum Likelihood method based  
220 on the JTT matrix-based model in MEGAX with 1000 bootstraps (Jones *et al.*, 1992).  
221 The tree with the highest log likelihood was shown. The two more distant effectors  
222 PITG\_16428 and PITG\_09577, served as an outgroup.

223

### 224 ***P. infestans* isolates and Detach Leaf Assay (DLA)**

225

226 The *P. infestans* isolates used in this study (90128, IPO-C and NL08645) were  
227 retrieved from our in-house collection. Isolates were grown at 15°C on solid rye  
228 medium in the dark (Caten & Jinks, 1968). After two weeks, sporulating mycelium  
229 was flooded with 20 mL of ice-cold water, adjusted to 70 zoospores/μL and incubated  
230 at 4°C for 2-3 hours. After the incubation, the detached leaves were inoculated with  
231 10μL of the zoospore suspension on the abaxial side of the leaves. Detached leaves  
232 were inserted into wet floral foam. For each biological replicate the three leaflets from

233 four leaves from two independent plants were used. Twelve spots on each leaf were  
234 inoculated with the zoospore suspension and closed in a plastic bag, to maintain high  
235 humidity. The leaves were kept in a climate cell at 18°C for 5 days. Disease  
236 resistance was scored on a scale from 1 to 10 for each leaflet. 10=no symptoms;  
237 9=HR no larger than the inoculum droplet; 8=HR lesion of up to 0,5 cm diameter;  
238 7=diffuse lesions up to 1cm diameter, no sporulation, no water soaking; 5= lesions  
239 larger than 1 cm sometimes with water soaking, no sporulation; 4=large water  
240 soaked lesions with sporulation only visible through binoculars; 2= large lesions with  
241 macroscopically visible sporulation on one side of the leaflet; 1= large lesions with  
242 macroscopically visible sporulation on both sides of the leaflet.

243

#### 244 **Relative effector and *R* gene expression**

245

246 The *P. infestans* effectors used in this study are listed in Table **S3**. The different  
247 genotypes were inoculated with the different *P. infestans* isolates and samples were  
248 collected after 0, 3, 8, 24, 48, 72, 96 and 120 hours. Infected plant material with the  
249 different *P. infestans* isolates was collected and RNA was isolated using RNA  
250 Purification Kit (QIAGEN). The isolated RNA was converted into cDNA using the  
251 QuantiTect Reverse Transcription Kit (QIAGEN). The primers used in this study are  
252 listed in Table **S2**. The expression of the different effectors in the infected material  
253 was evaluated using RT-qPCR SYBR Green (Bio-Rad). The samples were heated to  
254 95°C for 2min. Then 40 cycles of 15sec at 95°C, 30sec at 60°C and 30sec at 72°C.  
255 Fluorescence was measured after each cycle. After the final amplification cycle a  
256 melting curve was calculated. Relative gene expression was calculated using the  $2^{-\Delta\Delta CT}$   
257 method (Livak & Schmittgen, 2001). The normalised gene expression was  
258 obtained by dividing the relative gene expression by the relative *P. infestans*  
259 elongation factor 2 gene (*ef2*) expression.

260

#### 261 **sgRNA and CRISPR-Cas9 construct design**

262

263 The CRISPOR web tool (<http://crispor.org>) was used to design the sgRNAs with  
264 lower off-target and higher on-target potentials (Concordet & Haeussler, 2018).

265



266 A Modular Cloning (MoClo) system based on the Golden Gate cloning technology  
267 was used to assemble the different sgRNAs and binary vectors as previously  
268 described for tomato mutagenesis (Engler *et al.*, 2008; Weber *et al.*, 2011). Briefly,  
269 each sgRNA was fused to the *Arabidopsis thaliana* U6-26 promoter as *AtU6-*  
270 *26::gRNA*. The Level 1 constructs *pICH47732-pNOS::NPTII::tOCS*, *pICH47742-*  
271 *p2x35S::hCas9::tNOS* and the linker *pICH41780* were used to build the Level 2  
272 vector *pICSL4723* (Werner *et al.*, 2012). The primers used for cloning the gRNAs are  
273 listed in Table **S2**.

274

## 275 **Results**

### 276 **Cloning and characterization of *Rpi-chc1.1***

277

278 The *S. chacoense* accession CHC543 from Bolivia is a previously described wild  
279 potato relative harbouring resistance to *P. infestans* (Vleeshouwers *et al.*, 2011a). To  
280 identify the genetic locus of resistance, the resistant seedling CHC543-5 was crossed  
281 with the susceptible seedling CHC544-5 to generate the F1 population 7650,  
282 consisting initially of 212 individuals. This population was challenged with *P. infestans*  
283 isolate 90128 in a detached leaf assay (DLA). A clear 1:1 segregation was observed,  
284 indicating the presence of a single dominant resistance gene which will henceforth be  
285 referred to as *Rpi-chc1*. CAPS markers from chromosome 10 were tested as this  
286 chromosome was known to harbour *Rpi-ber* from the related species *S. berthaultii*  
287 (Vossen *et al.*, 2013). The marker TG63 in chromosome 10 was indeed linked to the  
288 *Rpi-chc1* resistance. Successive fine mapping in a recombinant population  
289 representing 2357 individuals was performed using markers derived from RH89-39-  
290 16 BAC clones from chromosome 10 (PGSC) (The Potato Genome Sequencing  
291 Consortium, 2011; Sharma *et al.*, 2013). A narrow genetic window between markers  
292 RH106G03-T and RH97D21\_C21-4 was identified to contain *Rpi-chc1* (Fig. **1a**). To  
293 generate a physical map of the mapping interval, two Bacterial Artificial Chromosome  
294 (BAC) clones, B1 and B2, were selected from a BAC library that was derived from  
295 CHC543-5 genomic DNA. After sequencing the BAC clones, two NLR genes were  
296 identified in clone B1 and another six NLR in clone B2. Further fine-mapping revealed  
297 that only the last six were located within the mapping interval and only three (B2-1,  
298 B2-2 and B2-3) encoded complete NLR proteins (Fig. **1b**). The three candidates were

299 subcloned including their native 5' and 3' regulatory elements, and complementation  
300 analyses were performed in *N. benthamiana*. After two days, the agroinfiltrated area  
301 was challenged with *P. infestans* 90128. *Rpi-blb1*, which was shown to provide  
302 resistance to *P. infestans*, was used as a positive control. The leaves agroinfiltrated  
303 with candidate B2-3 and *Rpi-blb1* showed severely compromised pathogen growth,  
304 while leaves with candidates B2-1 and B2-2 were completely susceptible to *P.*  
305 *infestans* 90128 (Fig. **S2**). This result suggested that B2-3 was the gene in CHC543-  
306 5 that provides resistance to *P. infestans*. To verify this result, the three candidates  
307 B2-1, B2-2 and B2-3 were stably transformed into the susceptible *S. tuberosum* cv.  
308 'Désirée'. Indeed, only the events containing candidate B2-3 showed resistance to *P.*  
309 *infestans* (Fig. **1c**). Furthermore, we specifically targeted the B2-3 candidate with  
310 sgRNAs and CRISPR-Cas9 enzyme by stable transformation of the resistant  
311 CHC543-5 genotype with. The transformation events were challenged with *P.*  
312 *infestans* 90128 and IPO-C isolates, and 48% of the transformants became  
313 susceptible to both isolates (Fig. **1d**; Table **S4**). Therefore, we concluded that B2-3  
314 was the gene from CHC543-5 that was causal for late blight resistance. Henceforth,  
315 we will refer to gene B2-3 as *Rpi-chc1.1* as it is the first *Rpi-chc1* allele that is  
316 identified in *S. chacoense*.

317

### 318 **Identification of *Rpi-chc1.1* allelic variants**

319

320 In order to identify different *Rpi-chc1.1* allelic variants, we pursued an allele mining  
321 approach in several resistant and susceptible *S. chacoense*, *S. berthaultii*, *S.*  
322 *tarijense*, and *S. tuberosum* accessions. Homologous sequences were amplified  
323 using primers overlapping the start and stop codons of *Rpi-chc1.1*. The PCR  
324 fragments of the expected 3.9 kb size were cloned and sequenced, resulting in the  
325 identification of fifteen *Rpi-chc1.1*-like sequences. From the selected diploid  
326 accessions one or two sequence variants were identified, suggesting that indeed *Rpi-*  
327 *chc1* alleles were mined rather than paralogs. Phylogenetic analysis of the  
328 sequences showed strong sequence similarities among the alleles (94.6 – 100%  
329 identity). Even within this high identity range, the presence of four main clades was  
330 revealed (Fig. **2a**). In clade 1, the *Rpi-chc1.1* allele was found, together with three  
331 sequences from *S. berthaultii* that were (nearly) identical to each other, and a  
332 sequence from *S. tarijense*. From clade 1, together with *Rpi-chc1.1*, we selected one

333 sequence from *S. berthaultii* (94-2031) and the *S. tarijense* (TAR852-5) for  
334 complementation analysis. Transformation of the corresponding genes to susceptible  
335 Désirée plants showed that they provide resistance to *P. infestans* isolates 90128  
336 and IPO-C, like *Rpi-chc1.1* (Table **S5**). We therefore concluded that clade 1 contains  
337 functional alleles of *Rpi-chc1*. The *S. tarijense* allele will be referred to as *Rpi-tar1.1*.  
338 The *S. berthaultii* allele will be referred to as *Rpi-ber1.1* which matches to the  
339 previously described *Rpi-ber* and *Rpi-ber1* genes that were derived from the same  
340 accession (PI473331) at similar genetic positions (Rauscher *et al.*, 2006; Tan *et al.*,  
341 2010; Vossen *et al.*, 2013).

342

343 The allele mining in accession CHC543-5 resulted not only in the re-identification of  
344 the active *Rpi-chc1.1* but also in the identification a presumed allelic variant, which  
345 we will refer to as *Rpi-chc1.2*. To test if *Rpi-chc1.1* and *Rpi-chc1.2* were indeed  
346 alleles of the same gene, we tested *Rpi-chc1.2* specific markers in the recombinant  
347 population 6750 (CHC543-5 x CHC544-5). We found a perfect repulsion between  
348 *Rpi-chc1.2* and *Rpi-chc1.1*, strongly suggesting that both genes are allelic variants  
349 (Table **S6**). Additionally, this analysis proved that *Rpi-chc1.2* does not cause  
350 resistance against *P. infestans* 90128, even though *Rpi-chc1.2* is expressed during  
351 infection (Fig. **S3f**). The *Rpi-chc1.2* protein sequence clusters in clade 2 together with  
352 four identical sequences from *S. berthaultii*. Close to clade 2, we can observe clade  
353 3, which consisted of a *S. berthaultii*, a *S. tarijense* and a *S. tuberosum* allele from  
354 RH89-039-16, a diploid clone previously characterised as susceptible to *P. infestans*  
355 (Vleeshouwers *et al.*, 2011a). The clade 3 allele from *S. tarijense* contained an in  
356 frame stop codon, making it unlikely that this allele is producing an active resistance  
357 protein. Additionally, a fourth clade contained only *S. berthaultii* alleles. The allelic  
358 variants were numbered according to the clade in which they were found (i.e. *Rpi-*  
359 *ber1.1* from clade 1 and *Rpi-ber1.2* from clade 2, etc.) followed by an extension to  
360 indicate the genotype from which the allele was derived.

361

362 The mined *Rpi-chc1.1* variants contained between 1296 to 1303 amino acids (Fig.  
363 **2b**; Fig. **S4**) and the encoded proteins belong to the CNL-16 immune receptor family  
364 (Witek *et al.* 2016). Their CC domains contain the N terminal MADA motif, 4  
365 predicted  $\alpha$ -helices and the typical hhGRExE, but the distinctive EDVID motif was  
366 less conserved. The NB domain contains the characteristic P-loop or Kinase 1a

367 domain, the VYND motif, Kinase 2 domain or Walker B, and the Kinase 3a or RNBS-  
368 B. The ARC1 domain contains the RNBS-C, the Motif 3 and the GLPL motif; and the  
369 ARC2 contains the Motif 2, the RNBS-D and two copies of the MHDL motif. The LRR  
370 domain consists of 29 imperfect repeats. Both LRR3 and LRR4 contain a central  
371 VLDL motif which is conserved in the third LRR of most functional NLRs.

372

373 **Rpi-chc1.1 recognises the RXLR PexRD12 effector family from *P.***  
374 ***infestans***

375

376 To understand the resistance mechanism of the *S. chacoense* CHC543-5 accession,  
377 we searched for the effector recognised by Rpi-chc1.1. A collection of ninety *P.*  
378 *infestans* extracellular (Pex) proteins in a PVX agroinfectious vector, of which 54  
379 contained the RXLR-DEER motif (PexRD), was screened. Individual clones from the  
380 Pex collection were co-agroinfiltrated with *Rpi-chc1.1* in *N. benthamiana* leaves. As a  
381 positive control, we used a mix of the *R3a/AVR3a* R gene effector pair which is  
382 known to trigger a strong hypersensitive response (HR) in *N. benthamiana* leaves.  
383 Only two effectors from the Pex collection were able to trigger an *Rpi-chc1.1*  
384 dependent HR, PexRD12-1 and PexRD12-2 (PITG\_16233 and PITG\_16240,  
385 respectively) (Fig. 3a). Neither the inactive paralogs B2-1 and B2-2 nor R3a  
386 produced an HR upon co-agroinfiltration with PexRD12. These results showed that  
387 PexRD12 is specifically recognised by Rpi-chc1.1. We could further confirm this  
388 finding using transgenic Désirée potato plants that were transformed with *Rpi-chc1.1*.  
389 About half of this transgenic population showed late blight resistance while the other  
390 half was susceptible, probably due to impaired transgene expression. Interestingly,  
391 the plants that showed late blight resistance also showed PexRD12 recognition, while  
392 the susceptible transgenic plants did not show any response upon PexRD12  
393 agroinfiltration (Table S7). We sought for further evidence that PexRD12 was indeed  
394 causing a-virulence on *Rpi-chc1.1* expressing plants. In a field trial with natural  
395 infection, we found isolates that were virulent on plants containing *Rpi-chc1.1*. The  
396 infected material was collected and used for gene expression analysis via RT-qPCR.  
397 The expression of PexRD12 was significantly reduced in the *Rpi-chc1.1* resistance  
398 breaking isolates, while other effectors such as *AVRsto1* were normally expressed.  
399 Reciprocally, we found that *Rpi-sto1* breaking isolates still expressed PexRD12

400 normally (Fig. **3b**). Altogether, these results suggest that PexRD12 corresponds to  
401 *AVRchc1.1*.

402

### 403 **The PexRD12/31 superfamily is a complex *P. infestans* RXLR effector family**

404

405 Using Blast analyses of the T30-4 proteome, we found 9 homologs of PexRD12 in  
406 the *P. infestans* T30-4 genome. Additionally, we found that PexRD12 proteins had  
407 strong homology with 9 members of the PexRD31 family and two additional, more  
408 distantly related sequences (Table **S3**). These 20 effectors are encoded by clusters  
409 of paralogs mainly in three supercontigs (Fig. **S5**) and will henceforth be referred to  
410 as the PexRD12/31 superfamily (see also Petre *et al.*, 2020). All PexRD12/31  
411 effectors are small proteins that include a signal peptide in the N-terminus, an  
412 effector domain in the C-terminus, and the conserved RXLR and EER motifs in the  
413 centre; except for PITG\_16243 and PITG\_09577 which contain an RXXR-EER and  
414 RXXLR-EER motifs, respectively (Fig. **4a**).

415

416 The alignment of the protein sequences and the phylogenetic analysis of the  
417 PexRD12/31 superfamily members resulted in five main clades (Fig. **4a**). Two highly  
418 homologous clades can be distinguished to form the PexRD12 family, PexRD12-A1  
419 and PexRD12-A2. The clade PexRD12-A2 also includes truncated versions which  
420 partly or completely miss the effector domain. In addition, two related clades  
421 constitute the PexRD31 family, PexRD31-B and PexRD31-C. Additionally,  
422 PITG\_16428 and PITG\_09577 were much less related and are together referred to  
423 as PexRD12/31 group D.

424

425 To determine the degree to which PexRD12/31 members are expressed *in planta*, as  
426 observed for other AVR effectors of *P. infestans* (Vleeshouwers *et al.*, 2011b;  
427 Rietman *et al.*, 2012), we tested their expression during infection with quantitative  
428 PCR on cDNA using clade A, B and C specific primers. The relative expression was  
429 calculated and normalised for the relative amount of *P. infestans*. Three different *P.*  
430 *infestans* isolates were evaluated at different time points after inoculation of different  
431 susceptible potato genotypes (Fig. **S3a-d**). In all the tested genotypes, PexRD12  
432 showed the highest relative expression. In two isolates a maximum expression was

433 found from 4 to 24 hours after inoculation and expression remained high till after 48  
434 hours in all four isolates. The PexRD31-B effectors were expressed in 2 isolates but  
435 were rapidly downregulated in the first hours after inoculation with hardly any  
436 expression left. The expression of PexRD31-C was mostly undetectable along the  
437 inoculation time course.

438

### 439 **Rpi-chc1.2 recognises the RXLR PexRD31 effector family from *P.*** 440 ***infestans***

441

442 In order to describe the spectrum of effector recognition by different *Rpi-chc1* alleles,  
443 several representatives from each clade were selected and co-agroinfiltrated with  
444 different PexRD12/31 members in *N. benthamiana*. *Rpi-chc1.1\_543-5* and *Rpi-*  
445 *ber1.1\_94-2031-01* from clade 1, *Rpi-chc1.2\_543-5* and *Rpi-ber1.2\_493-7* from clade  
446 2, and *rpi-tub1-RH89-039-16* from clade 3 were selected. As a representation from  
447 each of the clades of the PexRD12/31 effector superfamily, we selected:  
448 PITG\_16245 (PexRD12-A1), PITG\_20934 (PexRD12-A2), PITG\_16235 (PexRD31-  
449 B), and PITG\_23069 (PexRD31-C). The different *Rpi-chc1* alleles were co-  
450 agroinfiltrated with the PexRD12/31 effectors in *N. benthamiana* leaves. Three days  
451 after agroinfiltration, we observed that the members from clade 1, *Rpi-chc1.1* and  
452 *Rpi-ber1.1*, specifically recognised both PexRD12-A1 and PexRD12-A2 effectors  
453 (Fig. **4b**). This result showed that *Rpi-chc1.1* and *Rpi-ber1.1* recognise multiple  
454 members of the PexRD12 family, suggesting that AVRchc1.1 is encoded by multiple  
455 redundant paralogs. On the other hand, *Rpi-chc1.2* and *Rpi-ber1.2* from clade 2,  
456 specifically recognised both PexRD31-B and PexRD31-C effectors (Fig. **4b**). This  
457 suggests that multiple PexRD31 paralogs correspond to AVRchc1.2. The selected  
458 allele from clade 3, *rpi-tub1.3\_RH89-039-16*, was not able to recognize any of the  
459 PexRD12/31 members (Fig. **4b**), showing that clade 3 encodes functionally more  
460 distant receptors, and is in agreement with the known susceptibility of RH89-039-16  
461 to *P. infestans* (Vleeshouwers *et al.*, 2008).

462

### 463 **The LRR domain of the *Rpi-chc1* variants determines the PexRD12/31** 464 **effector recognition specificity**

465

466 Since the allelic variants of *Rpi-chc1* could be divided into three activity groups, while  
467 having an amino acid identity up to 96%, they provide ideal tools to investigate the  
468 *Rpi-chc1* mechanism of recognition. Therefore, we performed progressive exchanges  
469 of the different receptor domains. The chimeric receptors were co-agroinfiltrated with  
470 the PexRD12/31 effectors in *N. benthamiana* leaves to evaluate their recognition  
471 specificity. First, we selected *Rpi-chc1.2* and *rpi-tub1.3\_RH89-039-16* as  
472 representatives of clade B and clade C, respectively. When aligning the protein  
473 sequences, 54 single amino acid polymorphisms (SAPs) were found and most of  
474 them were located in the LRR domain (Fig. **5a**). As previously mentioned, *Rpi-chc1.2*  
475 specifically recognises PexRD31-B and PexRD31-C, while *rpi-tub1.3\_RH89-039-16*  
476 does not recognise any of the PexRD12/31 effectors. When the complete *rpi-*  
477 *tub1.3\_RH89-039-16* LRR domain was exchanged for the *Rpi-chc1.2* LRR, the  
478 chimeric receptor RH::C2\_2-29 was able to recognise both PexRD31-B and  
479 PexRD31-C. Reciprocally, the exchange of the *Rpi-chc1.2* LRR for the *rpi-*  
480 *tub1.3\_RH89-039-16* in C2::RH\_2-29, led to the inability to recognise any of the  
481 PexRD12/31 effectors. This result demonstrates the importance of the LRR domain  
482 during the AVRchc1.2 recognition. Additional domain exchanges were performed in  
483 order to identify the essential LRR repeats for the effector recognition. The required  
484 LRR repeats for the AVRchc1.2 recognition could be narrowed down with the  
485 construct RH::C2\_14-19 to nine amino acid polymorphisms (Fig. **5a**). Due to the  
486 absence of polymorphisms in the LRR repeats 14 and 15, we can conclude that only  
487 LRR repeats from 16 to 19 are required to activate the *rpi-tub1.3\_RH89-039-16* allele  
488 to recognise AVRchc1.2. Interestingly, the majority of these nine amino acid  
489 polymorphisms are particularly situated in the solvent exposed domain (xxLxLxxxx) of  
490 every LRR repeat. The exchange of any of the solvent exposed residues for the  
491 residues present in the inactive allele led to the partial or complete loss of effector  
492 recognition (Fig. **5b**).

493

494 To understand the difference in effector recognition specificity between *Rpi-chc1.1*  
495 and *Rpi-chc1.2*, and to explore the possibility to combine both recognitions in one  
496 receptor, we performed a similar progressive domain exchange approach between  
497 *Rpi-chc1.1* and *Rpi-chc1.2* (Fig. **6**). The exchange of the LRR domain in the chimeric  
498 receptors C1::C2\_8-29 and C2::C1\_8-29 led to a shift in effector recognition, from  
499 AVRchc1.1 to AVRchc1.2. Further exchanges revealed that the LRR repeats 14 to 23

500 from Rpi-chc1.2 led to an opposite effector recognition pattern as the chimeric  
501 receptor C1::C2\_14-23 was able to only recognise AVRchc1.2. With reciprocal  
502 domain exchanges of Rpi-chc1.1 into Rpi-chc1.2, we found that LRR repeats 8 to 29,  
503 led to AVRchc1.1 recognition. In an attempt to further reduce the length of the  
504 exchanged sequence, the recognition of AVRchc1.1 resulted in partial (C2::C1\_8-25  
505 and C2::C1\_8-23) or complete (C2::C1\_14-25 and C2::C1\_14-23) loss of recognition.  
506 Especially, when comparing the receptors C2::C1\_8-29 and C2::C1\_8-25, already  
507 the modification of the last five SAPs led to the reduced recognition of AVRchc1.1.  
508 But, apparently not only the last LRR repeats are involved in the effector recognition.  
509 Also the first LRR repeats, from 8 to 14, are also important for AVRchc1.1 recognition  
510 as C2::C1\_8-25 was able to partially recognise AVRchc1.1, while C2::C1\_14-25 did  
511 not trigger any HR. We conclude that the LRR repeats 8 to 29 in Rpi-chc1.1 are  
512 important for the AVRchc1.1 recognition, which overlaps with LRR repeats 16-19  
513 from Rpi-chc1.2 which were required for AVRchc1.2 recognition.

## 514 Discussion

515

516 In this study, we identified *Rpi-chc1.1* and 15 additional allelic variants from *S.*  
517 *berthaultii*, *S. tarijense* and *S. tuberosum*. Phylogenetic analysis of the encoded  
518 protein sequences revealed four clades. These four clades were not only supported  
519 by sequence similarity but also by differences in effector and *P. infestans* recognition.  
520 Clade 1 genes encode receptors that recognise PexRD12 effectors and includes the  
521 active orthologs *Rpi-chc1.1*, *Rpi-ber1.1* and *Rpi-tar1.1* (Fig. 2, 3). Clade 2 receptors  
522 could be distinguished by the recognition of the PexRD31 effectors (Fig. 4).  
523 Receptors encoded by clades 3 and 4 do not recognise PexRD12/31 effectors and  
524 no other activity has been found. Interestingly, clade 3 alleles are also present in  
525 domesticated potato clones that are susceptible to late blight; e.g. RH89-039-16 (Fig.  
526 2) and the varieties Colomba and Altus (unpublished data), implying that the encoded  
527 receptors are not able to effectively provide resistance against *P. infestans*.

528

529 *Rpi-ber1.1\_94-2031-01* was derived from the same accession as the previously  
530 described *Rpi-ber* (Rauscher *et al.*, 2006; Vossen *et al.*, 2009; Tan *et al.*, 2010), and  
531 *Rpi-ber1* genes (Park *et al.*, 2009). In these four studies, *Rpi-ber* and *Rpi-ber1*  
532 mapped close to marker TG63 but slightly different genetic positions were reported.



533 The population from Park *et al.* was quite small and a single recombination event  
534 may have caused the deviating genetic distance. In the case of Tan *et al.*, a single  
535 mis-phenotyping could explain the mapping of *Rpi-ber* distal to TG63. We therefore  
536 assume that *Rpi-ber* and *Rpi-ber1* are the same genes and adopt the *Rpi-ber1*  
537 naming as it is more consistent with current nomenclature for late blight resistance  
538 genes. *Rpi-ber2*, as described by Park *et al.*, was derived from the same accession  
539 that was used in our allele mining studies (BER493). We could not find a clade 1 *Rpi-*  
540 *chc1* allele from the BER493 accessions, which supports the idea that a more  
541 distantly related CNL16 member may be present that lacks sufficient match to the  
542 primer sequences, explaining the *Rpi-ber2* map position distal from TG63.

543

544 The presence of *Rpi-chc1* alleles in *S. tarijense* and *S. berthaultii* suggests a  
545 functional common ancestor existed before their speciation. However, it must be  
546 noted that the geographic locations where the accessions were found are close to  
547 each other in Bolivia. Since *S. chacoense*, *S. tarijense* and *S. berthaultii* are closely  
548 related, the presence of functional *Rpi-chc1* alleles in the three species might be a  
549 result from a recent species intercrossing.

550

551 Sequence similarity among the studied allelic variants correlated with their  
552 functionality, deduced by their ability to provide late blight resistance and *P. infestans*  
553 effector recognition (Fig. 3, 4). This is not the first described case of *R* gene allelic  
554 variants across *Solanum* species. *Rpi-blb1*, *Rpi-sto1* and *Rpi-pta1*, from the Mexican  
555 species *S. bulbocastanum*, *S. stoloniferum* and *S. papita* are allelic variants that  
556 recognise the same IpiO or PexRD6 *P. infestans* effector (Vleeshouwers *et al.*,  
557 2008). Among allelic variants of late blight resistance genes (i.e. *Rpi-blb3* and *Rpi-*  
558 *hjt1* that recognise AVR2 effectors), overlapping recognition specificities have been  
559 previously described (Champouret, 2010). Moreover, highly similar, but non-allelic *R*  
560 genes from the same CNL cluster had different recognition specificities, i.e. *Rpi-vnt1*,  
561 *Rpi-mcq1*, R9a, Ph-3 (Smilde *et al.*, 2005; Foster *et al.*, 2009; Zhang *et al.*, 2014; Jo  
562 *et al.*, 2015). In the current report, we describe for the first time that allelic variants of  
563 a late blight resistance gene show non-overlapping effector recognition specificities.  
564 Remarkably, the recognized effectors belonged to the same effector family, which is  
565 an intriguing finding in the light of host pathogen co-evolution.

566

567 When studying Rpi-chc1 protein domain structure, we identified most of the  
568 conserved CNL motifs. Remarkably, the MADA motif (Adachi *et al.*, 2019) was not  
569 located downstream of the starting methionine, but downstream of the second  
570 methionine in position 46 of the Rpi-chc1 protein. Further research is needed to show  
571 if either or both methionines are used as translational start codons. Interestingly, we  
572 recently cloned the functional late blight resistance gene from the late blight resistant  
573 variety Carolus (*Rpi-Carolus* gene; Hamed Salehian, unpublished data). Rpi-Carolus  
574 differed only at 7 amino acid positions from Rpi-ber1, but its N-terminus was shorter  
575 as a stop codon was present between the first two methionine codons. This strongly  
576 suggests that translation in Rpi-Carolus starts from the second methionine while  
577 retaining biological activity.

578  
579 In contrast to the relatively conserved N termini of the proteins encoded by the *Rpi-*  
580 *chc1* alleles, most interallelic sequence variation localised to the Leucine Rich  
581 Repeat regions. Through domain interchange between the *rpi-tub1.3\_RH89-039-16*  
582 and a *Rpi-chc1.2* alleles and between Rpi-chc1.1 and Rpi-chc1.2, we discovered that  
583 the LRR domain defines recognition specificity (Fig. 5, 6). Polymorphisms in the LRR  
584 of some NLR receptors were previously shown to determine the effector recognition  
585 specificity (Dodds *et al.*, 2001; Shen *et al.*, 2003; Catanzariti *et al.*, 2010; Krasileva *et*  
586 *al.*, 2010; Ravensdale *et al.*, 2012; Lindner *et al.* 2020). In one example, a domain  
587 exchange between Rx1 and Gpa2 converted the virus resistance into nematode  
588 resistance, and vice versa (Slootweg *et al.*, 2017). The recognition of both nematode  
589 and virus could not be combined into one chimeric receptor, as we also observed  
590 with Rpi-chc1.1 and Rpi-chc1.2. The reason for this is the overlap between the LRRs  
591 involved in recognition.

592  
593 Most of the amino acids in Rpi-chc1.2 that were required for AVRchc1.2 recognition  
594 are located in the LRR solvent exposed motif (xxLxLxxxx) and modification of any of  
595 the solvent exposed amino acids led to the partial or complete loss of PexRD31  
596 recognition (Fig. 5b). The co-requirement of these solvent exposed amino acids  
597 suggests that they are involved in recognition of a particular epitope. This  
598 observation, combined with the observation of unequal distribution of SAPs, allow us  
599 to hypothesise that *Rpi-chc1* alleles evolved through insertion of a stretch of DNA into  
600 the LRR domain rather than through accumulation of independent mutation. A similar

601 model of evolution was recently proposed for allelic variants of *Rpi-amr1* (Witek *et al.*,  
602 2020). Such insertions may happen through unequal crossing-over with paralog  
603 sequences or through retro-transposition. Interestingly, the evolution of integrated  
604 domains in *R* genes has been postulated to be caused by an unknown recombination  
605 or transposon independent translocation mechanism (Bailey *et al.*, 2018). The same  
606 mechanism may be active in LRR exchange to evolve recognition of non-integrated  
607 domains like guardees or decoys (Kourelis & van der Hoorn, 2018) or direct effector  
608 recognition.

609

610 Interestingly, some of the PexRD31 family members have been previously identified  
611 as one of the most rapidly diversifying and fast evolving RXLR effectors in the T30-4  
612 genome, with  $\omega$  values higher than 1.55 (Haas *et al.*, 2009). Additionally, several  
613 members of the PexRD12/31 superfamily have recently been characterised to target  
614 the host vesicle trafficking machinery by interacting with the vesicle associated  
615 membrane protein 72 (VAMP72) family (Petre *et al.*, 2020). Even though both  
616 PexRD12 and PexRD31 have the same or functionally similar host targets, they are  
617 differentially expressed during *P. infestans* infection. While PexRD12 is highly  
618 expressed in all the tested isolates, PexRD31 is expressed at low levels after contact  
619 with potato (Fig. **S3**). This would also explain why *Rpi-chc1.2* is not able to provide  
620 resistance against *P. infestans*, since most of the isolates have low expression levels  
621 of *AVRchc1.2*. Consequently, clade A (PexRD12) may have evolved to avoid  
622 detection by *Rpi-chc1.2* while retaining its targeting of the vesicle trafficking  
623 machinery.

624

625 Another step in the co-evolution between *Rpi-chc1.1* and the PexRD12/31 family was  
626 found by analysing the effector expression in plants expressing *Rpi-chc1.1*. The  
627 isolates that overcome the *Rpi-chc1.1* resistance no longer express PexRD12, while  
628 the expression in untransformed Désirée plants was normal and comparable to the  
629 expression of *AVRsto1* (Fig. **3b**). Similarly, evasion of recognition through  
630 transcriptional suppression, was previously observed in plants expressing *Rpi-vnt1*  
631 infected with *P. infestans* (Pel, 2010). Once more, we confirmed the plasticity of the  
632 *P. infestans* effector secretion and the fast evolution capacity of some aggressive  
633 isolates to break down single *Rpi* resistances.

634

635 The introgression of single *R* genes is driving *P. infestans* to evolve and evade  
636 recognition. In order to durably deploy late blight resistance in agriculture, we need  
637 novel strategies informed by knowledge of disease resistance genes in varieties, their  
638 recognition specificities and the presence of the cognate effectors in the pathogen  
639 populations. Virulence information from the field must be rapidly translated to  
640 decision support systems (DSS) for the risk prediction and calculation of biocide  
641 spraying intervals. Additionally, DSS can be used to determine *R* gene composition  
642 of (novel) varieties to be deployed in the next season. To meet these requirements,  
643 novel breeding strategies are needed to rapidly tailor the *R* gene contents of the  
644 potato varieties to the pathogen populations. In current breeding schemes it takes  
645 10-15 years to select a late blight resistant potato variety. Moreover, susceptible  
646 varieties with dominant market shares will not be easy to replace. A system of  
647 varieties with flexible *R* gene content is needed. In other crops this has been  
648 accomplished through F1 hybrid varieties. In potato, this route has only recently been  
649 opened (Su *et al.*, 2020) and no hybrid potato varieties have reached the market yet.  
650 Proof of principle for flexible late blight resistance varieties produced through  
651 cisgenesis was provided several years ago (Haverkort *et al.*, 2016). Unfortunately,  
652 the EU legislation does not distinguish between cisgenic and transgenic products,  
653 making it impossible to market cisgenic varieties. Now, novel gene editing tools have  
654 become available, and legislation for their application in agriculture is still under  
655 debate. Knowledge as obtained in this study is essential to pursue such applications.  
656 We now know how inactive resistance genes from susceptible varieties could be  
657 repaired by replacing minimal fragments with the corresponding fragments of alleles  
658 from wild relatives. This would provide an unprecedented accuracy and speed which  
659 is not in introgression breeding.

660

## 661 **Acknowledgements**

662

663 The first part of this research was performed in the DuRPh project, funded by the  
664 Ministry of Agriculture, Nature and Food Quality in the Netherlands. The second part  
665 of the research was funded by the Ministry of Infrastructure and Water Management  
666 in the Netherlands through the NWO-TTW program Biotechnology and Safety  
667 (projectnumber 15815). We thank Jan de Boer and Adillah Tan for advice in selecting  
668 BAC clones and marker sequences from chr10. Evert Jacobsen and Clemens van

669 der Wiel are thanked for their advice about regulation and safety aspects of plant  
670 biotechnology. Sidrat Abdullah is thanked for testing late blight resistance of  
671 transgenic potato plants harbouring *Rpi-chc1* allelic variants. Last but not least, we  
672 thank Marjan Bergervoet, Gert van Arkel, Koen Pelgrom, Dirk Jan Huigen and Isolde  
673 Pereira for plant transformations, molecular biology assistance and plant  
674 maintenance.

675

## 676 **Data Availability**

677 All described sequences have been submitted top GenBank.

678

## 679 **Author contribution**

680

681 JV planned and designed the research; DML, MN and LK performed the majority of  
682 the experiments; SK provided the Pex-RD set; DML and JV wrote the manuscript; RV  
683 proofread the manuscript and provided the essential research environment. SA, HS  
684 and KS contributed by mapping, cloning and characterization of *Rpi-chc1* allelic  
685 variants. RS, AL and AAH contributed through the identification of AVRchc1 and their  
686 differential recognition specificities by *Rpi-chc1* allelic variants.

687

## 688 **References**

689

690 **Adachi H, Contreras MP, Harant A, Wu C, Derevnina L, Sakai T, Duggan C, Moratto**  
691 **E, Bozkurt TO, Maqbool A, et al. 2019.** An N-terminal motif in NLR immune receptors is  
692 functionally conserved across distantly related plant species. *eLife* **8**: e49956.

693 **Aguilera-Galvez C, Champouret N, Rietman H, Lin X, Wouters D, Chu Z, Jones JDG,**  
694 **Vossen JH, Visser RGF, Wolters PJ, et al. 2018.** Two different R gene loci co-evolved with  
695 Avr2 of *Phytophthora infestans* and confer distinct resistance specificities in potato. *Studies in*  
696 *Mycology* **89**: 105–115.

697 **Bailey PC, Schudoma C, Jackson W, Baggs E, Dagdas G, Haerty W, Moscou M,**  
698 **Krasileva KV. 2018.** Dominant integration locus drives continuous diversification of plant  
699 immune receptors with exogenous domain fusions. *Genome Biology* **19**: 23.

700 **Ballvora A, Ercolano MR, Weiss J, Meksem K, Bormann CA, Oberhagemann P,**  
701 **Salamini F, Gebhardt C. 2002.** The R1 gene for potato resistance to late blight  
702 (*Phytophthora infestans*) belongs to the leucine zipper/NBS/LRR class of plant resistance  
703 genes. *The Plant Journal* **30**: 361–371.

704 **Callaway E. 2013.** Pathogen genome tracks Irish potato famine back to its roots. *Nature*:  
705 nature.2013.13021.

- 706 **Catanzariti A-M, Dodds PN, Ve T, Kobe B, Ellis JG, Staskawicz BJ. 2010.** The AvrM  
707 Effector from Flax Rust Has a Structured C-Terminal Domain and Interacts Directly with the  
708 M Resistance Protein. *Molecular Plant-Microbe Interactions*® **23**: 49–57.
- 709 **Caten CE, Jinks JL. 1968.** Spontaneous variability of single isolates of *Phytophthora*  
710 *infestans*. I. Cultural variation. *Canadian Journal of Botany* **46**: 329–348.
- 711 **Champouret N. 2010.** Functional genomics of *Phytophthora infestans* effectors and *Solanum*  
712 resistance genes. PhD thesis, Wageningen University. <https://edepot.wur.nl/138174>
- 713 **Concordet J-P, Haeussler M. 2018.** CRISPOR: intuitive guide selection for CRISPR/Cas9  
714 genome editing experiments and screens. *Nucleic Acids Research* **46**: W242–W245.
- 715 **Dodds PN, Lawrence GJ, Ellis JG. 2001.** Six Amino Acid Changes Confined to the  
716 Leucine-Rich Repeat  $\beta$ -Strand/ $\beta$ -Turn Motif Determine the Difference between the P and P2  
717 Rust Resistance Specificities in Flax. *The Plant Cell* **13**: 163–178.
- 718 **Domazakis E, Lin X, Aguilera-Galvez C, Wouters D, Bijsterbosch G, Wolters PJ,**  
719 **Vleeshouwers VGAA. 2017.** Effectoromics-Based Identification of Cell Surface Receptors in  
720 Potato. In: Shan L, He P, eds. *Methods in Molecular Biology. Plant Pattern Recognition*  
721 *Receptors*. New York, NY: Springer New York, 337–353.
- 722 **Engler C, Kandzia R, Marillonnet S. 2008.** A One Pot, One Step, Precision Cloning  
723 Method with High Throughput Capability (HA El-Shemy, Ed.). *PLoS ONE* **3**: e3647.
- 724 **Foster SJ, Park T-H, Pel M, Brigneti G, Śliwka J, Jagger L, van der Vossen E, Jones**  
725 **JDG. 2009.** Rpi-vnt1.1 , a Tm-2 Homolog from *Solanum venturii* , Confers Resistance to  
726 Potato Late Blight. *Molecular Plant-Microbe Interactions*® **22**: 589–600.
- 727 **Fry W. 2008.** *Phytophthora infestans*: the plant (and R gene) destroyer. *Molecular Plant*  
728 *Pathology* **9**: 385–402.
- 729 **Goss EM, Press CM, Grünwald NJ. 2013.** Evolution of RXLR-Class Effectors in the  
730 Oomycete Plant Pathogen *Phytophthora ramorum* (A Palsson, Ed.). *PLoS ONE* **8**: e79347.
- 731 **Haas BJ, Kamoun S, Zody MC, Jiang RHY, Handsaker RE, Cano LM, Grabherr M,**  
732 **Kodira CD, Raffaele S, Torto-Alalibo T, et al. 2009.** Genome sequence and analysis of the  
733 Irish potato famine pathogen *Phytophthora infestans*. *Nature* **461**: 393–398.
- 734 **Haverkort AJ, Boonekamp PM, Hutten R, Jacobsen E, Lotz LAP, Kessel GJT, Vossen**  
735 **JH, Visser RGF. 2016.** Durable Late Blight Resistance in Potato Through Dynamic Varieties  
736 Obtained by Cisgenesis: Scientific and Societal Advances in the DuRPh Project. *Potato*  
737 *Research* **59**: 35–66.
- 738 **Huang S, Van Der Vossen EAG, Kuang H, Vleeshouwers VGAA, Zhang N, Borm TJA,**  
739 **Van Eck HJ, Baker B, Jacobsen E, Visser RGF. 2005.** Comparative genomics enabled the  
740 isolation of the R3a late blight resistance gene in potato: Cloning the potato late blight R3a  
741 gene by synteny. *The Plant Journal* **42**: 251–261.
- 742 **Huang S, Vleeshouwers VGAA, Werij JS, Hutten RCB, van Eck HJ, Visser RGF,**  
743 **Jacobsen E. 2004.** The R3 Resistance to *Phytophthora infestans* in Potato is Conferred by

- 744 Two Closely Linked R Genes with Distinct Specificities. *Molecular Plant-Microbe*  
745 *Interactions*® **17**: 428–435.
- 746 **Jo K-R, Visser RGF, Jacobsen E, Vossen JH. 2015.** Characterisation of the late blight  
747 resistance in potato differential MaR9 reveals a qualitative resistance gene, R9a, residing in a  
748 cluster of Tm-2 2 homologs on chromosome IX. *Theoretical and Applied Genetics* **128**: 931–  
749 941.
- 750 **Jo K-R, Zhu S, Bai Y, Hutten RCB, Kessel GJT, Vleeshouwers VGAA, Jacobsen E,**  
751 **Visser RGF, Vossen JH. 2016.** Problematic Crops: 1. Potatoes: Towards Sustainable Potato  
752 Late Blight Resistance by Cisgenic R Gene Pyramiding. In: Collinge DB, ed. *Plant Pathogen*  
753 *Resistance Biotechnology*. Hoboken, NJ: John Wiley & Sons, Inc, 171–191.
- 754 **Jones DT, Taylor WR, Thornton JM. 1992.** The rapid generation of mutation data matrices  
755 from protein sequences. *Bioinformatics* **8**: 275–282.
- 756 **Jupe F, Witek K, Verweij W, Śliwka J, Pritchard L, Etherington GJ, Maclean D, Cock**  
757 **PJ, Leggett RM, Bryan GJ, et al. 2013.** Resistance gene enrichment sequencing (RenSeq)  
758 enables reannotation of the NB-LRR gene family from sequenced plant genomes and rapid  
759 mapping of resistance loci in segregating populations. *The Plant Journal* **76**: 530–544.
- 760 **Kourelis J, van der Hoorn RAL. 2018.** Defended to the Nines: 25 Years of Resistance Gene  
761 Cloning Identifies Nine Mechanisms for R Protein Function. *The Plant Cell* **30**: 285–299.
- 762 **Krasileva KV, Dahlbeck D, Staskawicz BJ. 2010.** Activation of an Arabidopsis Resistance  
763 Protein Is Specified by the in Planta Association of Its Leucine-Rich Repeat Domain with the  
764 Cognate Oomycete Effector. *The Plant Cell* **22**: 2444–2458.
- 765 **Kumar S, Stecher G, Li M, Knyaz C, Tamura K. 2018.** MEGA X: Molecular Evolutionary  
766 Genetics Analysis across Computing Platforms (FU Battistuzzi, Ed.). *Molecular Biology and*  
767 *Evolution* **35**: 1547–1549.
- 768 **Leister D. 2004.** Tandem and segmental gene duplication and recombination in the evolution  
769 of plant disease resistance genes. *Trends in Genetics* **20**: 116–122.
- 770 **Li G, Huang S, Guo X, Li Y, Yang Y, Guo Z, Kuang H, Rietman H, Bergervoet M,**  
771 **Vleeshouwers VGGA, et al. 2011.** Cloning and Characterization of R3b; Members of the R3  
772 Superfamily of Late Blight Resistance Genes Show Sequence and Functional Divergence.  
773 *Molecular Plant-Microbe Interactions*® **24**: 1132–1142.
- 774 **Lindner S, Keller B, Singh SP, Hasenkamp Z, Jung E, Müller MC, Bourras S and Keller**  
775 **B 2020.** Single residues in the LRR domain of the wheat PM3A immune receptor can control  
776 the strength and the spectrum of the immune response. *Plant Journal* **104**: 200–214.  
777
- 778 **Livak KJ, Schmittgen TD. 2001.** Analysis of Relative Gene Expression Data Using Real-  
779 Time Quantitative PCR and the 2– $\Delta\Delta$ CT Method. *Methods* **25**: 402–408.
- 780 **Lokossou AA, Park T, van Arkel G, Arens M, Ruyter-Spira C, Morales J, Whisson SC,**  
781 **Birch PRJ, Visser RGF, Jacobsen E, et al. 2009.** Exploiting Knowledge of R/Avr Genes to  
782 Rapidly Clone a New LZ-NBS-LRR Family of Late Blight Resistance Genes from Potato  
783 Linkage Group IV. *Molecular Plant-Microbe Interactions*® **22**: 630–641.

- 784 **McBride KE, Summerfelt KR. 1990.** Improved binary vectors for *Agrobacterium*-mediated  
785 plant transformation. *Plant Molecular Biology* **14**: 269–276.
- 786 **Mcdowell JM, Simon SA. 2006.** Recent insights into R gene evolution. *Molecular Plant*  
787 *Pathology* **7**: 437–448.
- 788 **Park T-H, Foster S, Brigneti G, Jones JDG. 2009.** Two distinct potato late blight resistance  
789 genes from *Solanum berthaultii* are located on chromosome 10. *Euphytica* **165**: 269–278.
- 790 **Pel MA. 2010.** *Mapping, isolation and characterization of genes responsible for late blight*  
791 *resistance in potato*. PhD thesis, Wageningen University. <https://edepot.wur.nl/138132>
- 792 **Pel MA, Foster SJ, Park T-H, Rietman H, van Arkel G, Jones JDG, Van Eck HJ,**  
793 **Jacobsen E, Visser RGF, Van der Vossen EAG. 2009.** Mapping and Cloning of Late Blight  
794 Resistance Genes from *Solanum venturii* Using an Interspecific Candidate Gene Approach.  
795 *Molecular Plant-Microbe Interactions*® **22**: 601–615.
- 796 **Petre B, Contreras MP, Bozkurt TO, Schattat MH, Sklenar J, Schornack S, Abd-El-**  
797 **Haliem A, Castells-Graells R, Lozano-Duran R, Dagdas YF, et al. 2020.** *Host-interactor*  
798 *screens of Phytophthora infestans RXLR proteins reveal vesicle trafficking as a major*  
799 *effector-targeted process*. *Plant Biology*.
- 800 **Rauscher GM, Smart CD, Simko I, Bonierbale M, Mayton H, Greenland A, Fry WE.**  
801 **2006.** Characterization and mapping of Rpi-ber , a novel potato late blight resistance gene  
802 from *Solanum berthaultii*. *Theoretical and Applied Genetics* **112**: 674–687.
- 803 **Ravensdale M, Bernoux M, Ve T, Kobe B, Thrall PH, Ellis JG, Dodds PN. 2012.**  
804 *Intramolecular Interaction Influences Binding of the Flax L5 and L6 Resistance Proteins to*  
805 *their AvrL567 Ligands* (J-R Xu, Ed.). *PLoS Pathogens* **8**: e1003004.
- 806 **Rietman H, Bijsterbosch G, Cano LM, Lee H-R, Vossen JH, Jacobsen E, Visser RGF,**  
807 **Kamoun S, Vleeshouwers VGAA. 2012.** Qualitative and Quantitative Late Blight Resistance  
808 in the Potato Cultivar Sarpo Mira Is Determined by the Perception of Five Distinct RXLR  
809 Effectors. *Molecular Plant-Microbe Interactions*® **25**: 910–919.
- 810 **Sharma SK, Bolser D, de Boer J, Sønderkær M, Amoros W, Carboni MF, D’Ambrosio**  
811 **JM, de la Cruz G, Di Genova A, Douches DS, et al. 2013.** Construction of Reference  
812 Chromosome-Scale Pseudomolecules for Potato: Integrating the Potato Genome with Genetic  
813 and Physical Maps. *G3&#58; Genes/Genomes/Genetics* **3**: 2031–2047.
- 814 **Shen Q-H, Zhou F, Bieri S, Haizel T, Shirasu K, Schulze-Lefert P. 2003.** Recognition  
815 Specificity and RAR1/SGT1 Dependence in Barley Mla Disease Resistance Genes to the  
816 Powdery Mildew Fungus. *The Plant Cell* **15**: 732–744.
- 817 **Sievers F, Wilm A, Dineen D, Gibson TJ, Karplus K, Li W, Lopez R, McWilliam H,**  
818 **Remmert M, Söding J, et al. 2011.** Fast, scalable generation of high-quality protein  
819 multiple sequence alignments using Clustal Omega. *Molecular Systems Biology* **7**: 539.
- 820 **Slootweg E, Koropacka K, Roosien J, Dees R, Overmars H, Lankhorst RK, van Schaik**  
821 **C, Pomp R, Bouwman L, Helder J, et al. 2017.** Sequence Exchange between Homologous  
822 NB-LRR Genes Converts Virus Resistance into Nematode Resistance, and Vice Versa. *Plant*  
823 *Physiology* **175**: 498–510.



- 824 **Smilde WD, Brigneti G, Jagger L, Perkins S, Jones JDG. 2005.** Solanum mochiquense  
825 chromosome IX carries a novel late blight resistance gene Rpi-moc1. *Theoretical and Applied*  
826 *Genetics* **110**: 252–258.
- 827 **Song J, Bradeen JM, Naess SK, Raasch JA, Wielgus SM, Haberlach GT, Liu J, Kuang**  
828 **H, Austin-Phillips S, Buell CR, et al. 2003.** Gene RB cloned from Solanum bulbocastanum  
829 confers broad spectrum resistance to potato late blight. *Proceedings of the National Academy*  
830 *of Sciences* **100**: 9128–9133.
- 831 **Su Y, Viquez-Zamora M, den Uil D, Sinnige J, Kruyt H, Vossen J, Lindhout P, van**  
832 **Heusden S. 2020.** Introgression of Genes for Resistance against Phytophthora infestans in  
833 Diploid Potato. *American Journal of Potato Research* **97**: 33–42.
- 834 **Tan MYA, Hutten RCB, Visser RGF, van Eck HJ. 2010.** The effect of pyramiding  
835 Phytophthora infestans resistance genes R Pi-mcd1 and R Pi-ber in potato. *Theoretical and*  
836 *Applied Genetics* **121**: 117–125.
- 837 **The Potato Genome Sequencing Consortium. 2011.** Genome sequence and analysis of the  
838 tuber crop potato. *Nature* **475**: 189–195.
- 839 **Vleeshouwers VG, Finkers R, Budding D, Visser M, Jacobs MM, van Berloo R, Pel M,**  
840 **Champouret N, Bakker E, Krenek P, et al. 2011a.** SolRgene: an online database to explore  
841 disease resistance genes in tuber-bearing Solanum species. *BMC Plant Biology* **11**: 116.
- 842 **Vleeshouwers VGAA, Raffaele S, Vossen JH, Champouret N, Oliva R, Segretin ME,**  
843 **Rietman H, Cano LM, Lokossou A, Kessel G, et al. 2011b.** Understanding and Exploiting  
844 Late Blight Resistance in the Age of Effectors. *Annual Review of Phytopathology* **49**: 507–  
845 531.
- 846 **Vleeshouwers VGAA, Rietman H, Krenek P, Champouret N, Young C, Oh S-K, Wang**  
847 **M, Bouwmeester K, Vosman B, Visser RGF, et al. 2008.** Effector Genomics Accelerates  
848 Discovery and Functional Profiling of Potato Disease Resistance and Phytophthora Infestans  
849 Avirulence Genes (HA El-Shemy, Ed.). *PLoS ONE* **3**: e2875.
- 850 **Vossen JH, van Arkel G, Bergervoet M, Jo K-R, Jacobsen E, Visser RGF. 2016.** The  
851 Solanum demissum R8 late blight resistance gene is an Sw-5 homologue that has been  
852 deployed worldwide in late blight resistant varieties. *Theoretical and Applied Genetics* **129**:  
853 1785–1796.
- 854 **Vossen JH, Dezhsetan S, Esselink D, Arens M, Sanz MJ, Verweij W, Verzaux E, van der**  
855 **Linden C. 2013.** Novel applications of motif-directed profiling to identify disease resistance  
856 genes in plants. *Plant Methods* **9**: 37.
- 857 **Vossen JH, Nijenhuis M, Arens M, Van Der Vossen EAG, Jacobsen E, Visser RGF.**  
858 **2009.** Cloning and exploitation of a functional R gene from Solanum chacoense. Patent  
859 application WO2011034433 A1. Published by the world intellectual property organization 18  
860 September 2009
- 861 **van der Vossen EAG, Gros J, Sikkema A, Muskens M, Wouters D, Wolters P, Pereira A,**  
862 **Allefs S. 2005.** The Rpi-blb2 gene from Solanum bulbocastanum is an Mi-1 gene homolog  
863 conferring broad-spectrum late blight resistance in potato: Isolation of the late blight  
864 resistance gene Rpi-blb2. *The Plant Journal* **44**: 208–222.

865 **van de Vossen BTLH, Prodhomme C, van Arkel G, van Gent-Pelzer MPE,**  
866 **Bergervoet M, Brankovics B, Przetakiewicz J, Visser RGF, van der Lee TAJ, Vossen**  
867 **JH. 2019.** The *Synchytrium endobioticum* AvrSen1 Triggers a Hypersensitive Response in  
868 Sen1 Potatoes While Natural Variants Evade Detection. *Molecular Plant Microbe*  
869 *Interactions* **32**: 1536-1546.

870 **van der Vossen E, Sikkema A, Hekkert B te L, Gros J, Stevens P, Muskens M, Wouters**  
871 **D, Pereira A, Stiekema W, Allefs S. 2003.** An ancient R gene from the wild potato species  
872 *Solanum bulbocastanum* confers broad-spectrum resistance to *Phytophthora infestans* in  
873 cultivated potato and tomato. *The Plant Journal* **36**: 867–882.

874 **Weber E, Engler C, Gruetzner R, Werner S, Marillonnet S. 2011.** A Modular Cloning  
875 System for Standardized Assembly of Multigene Constructs (J Peccoud, Ed.). *PLoS ONE* **6**:  
876 e16765.

877 **Werner S, Engler C, Weber E, Gruetzner R, Marillonnet S. 2012.** Fast track assembly of  
878 multigene constructs using Golden Gate cloning and the MoClo system. *Bioengineered* **3**: 38–  
879 43.

880 **Witek K, Jupe F, Witek A. et al. (2016).** Accelerated cloning of a potato late blight–  
881 resistance gene using RenSeq and SMRT sequencing. *Nature Biotechnology* **34**, 656–660

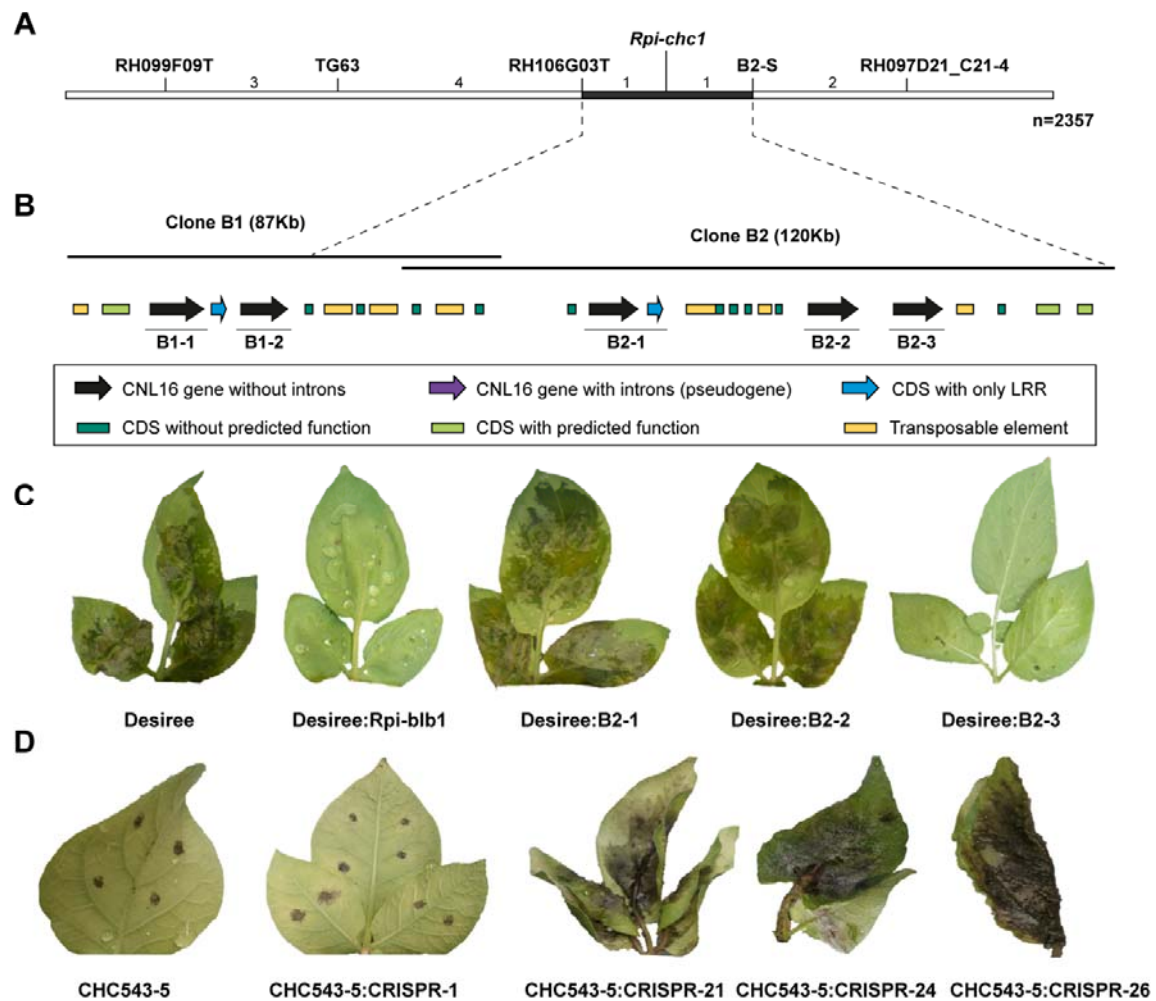
882

883 **Witek K, Lin X, Karki HS, Jupe F, Witek AI, Steuernagel B, Stam R, van Oosterhout C,**  
884 **Fairhead S, Cocker JM, et al. 2020.** A complex resistance locus in *Solanum americanum*  
885 recognizes a conserved *Phytophthora* effector. *BioRxiv* 2020.05.15.095497 doi:  
886 <https://doi.org/10.1101/2020.05.15.095497>

887 **Zhang C, Liu L, Wang X, Vossen J, Li G, Li T, Zheng Z, Gao J, Guo Y, Visser RGF, et**  
888 **al. 2014.** The Ph-3 gene from *Solanum pimpinellifolium* encodes CC-NBS-LRR protein  
889 conferring resistance to *Phytophthora infestans*. *Theoretical and Applied Genetics* **127**: 1353–  
890 1364.

891 **Zhu S, Vossen JH, Bergervoet M, Nijenhuis M, Kodde L, Vleeshouwers VGGA, Visser**  
892 **RGF, Jacobsen E. 2015.** An updated conventional- and a novel GM potato late blight R gene  
893 differential set for virulence monitoring of *Phytophthora infestans*. *Euphytica* **202**: 219–234

894



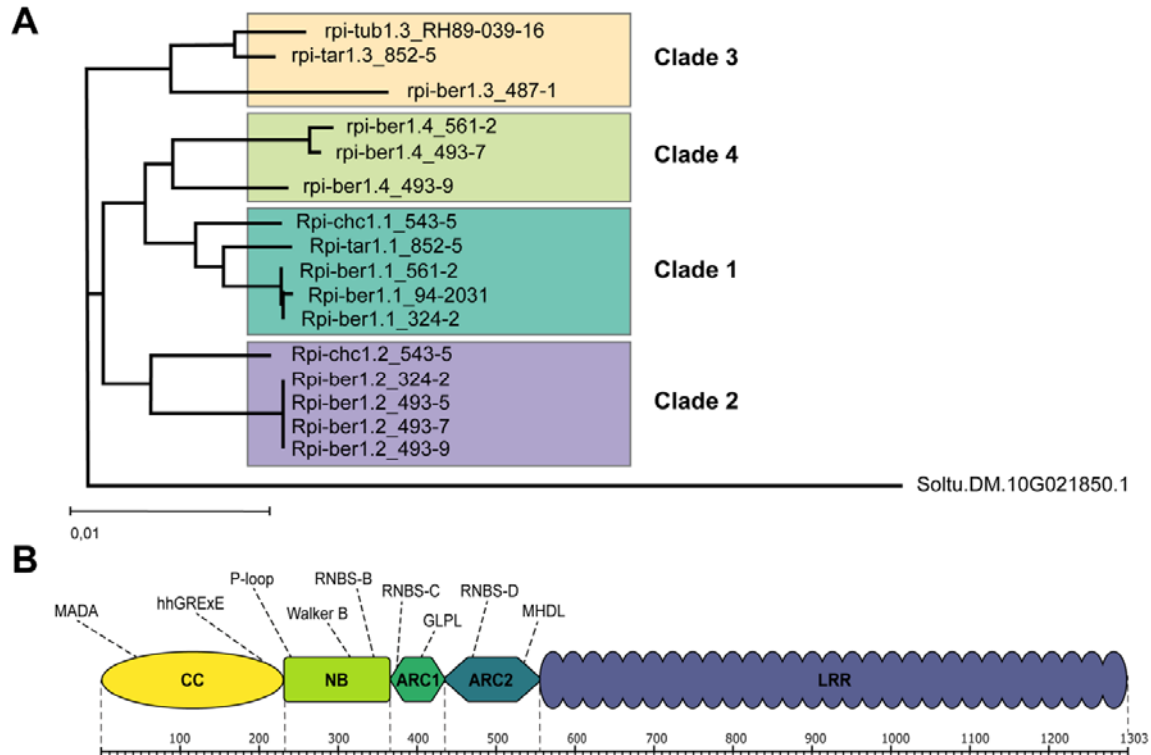
895 **Figures:**

896

897 **Fig. 1.** Map based cloning of *Rpi-chc1.1*.

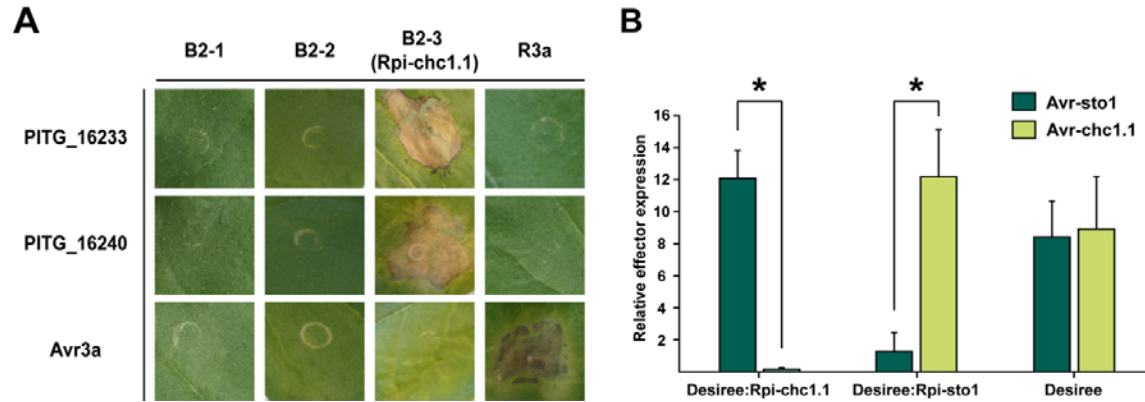
898 (A) Genetic map of *P. infestans* (isolate 90128) resistance from CHC543-5. The  
 899 number between the markers represents the number of recombinants found in a  
 900 population derived from 2357 seedlings. Markers starting with RH were derived from  
 901 BAC end sequences generated by PGSC. Marker B2-S represents the BAC end  
 902 marker from clone 2. The black horizontal line represents the interval of *Rpi-chc1.1*.  
 903 (B) Two BAC clones were isolated to generate the physical map. Annotation revealed  
 904 the presence of NB-LRR genes, genes with or without predicted function and  
 905 transposable elements. Three complete NB-LRR (B2-1, B2-2 and B2-3) genes  
 906 between flanking markers RH106G03T and B2-S were selected as candidates. (C)  
 907 The three candidates were stably transformed into the potato variety Desiree. After  
 908 inoculation with isolate 90128, only the candidate B2-3 was able to provide  
 909 resistance. Untransformed Desiree and Desiree plants stably transformed with *Rpi-*  
 910 *ubl1* were used as negative and positive controls, respectively. (D) CRISPR-Cas9  
 911 constructs were designed to specifically target candidate B2-3 and stably  
 912 transformed in the *S. chacoense* 543-5 resistant genotype. Transgenic plants with

913 B2-3 knock-outs were susceptible to *P. infestans* 90128 and IPO-C isolates.  
 914 Transgenic plants without mutations in the B2-3 candidate and untransformed  
 915 CHC543-5 were used as a control.



916  
 917 **Fig. 2. *Rpi-chc1* allele mining.**  
 918 (A) Sixteen *Rpi-chc1.1*-like sequences were cloned from eleven different diploid  
 919 *Solanum* accessions. From seven accessions two variants were identified. From four  
 920 accessions only one variant was found, suggesting that the second allele did not  
 921 match the PCR primers. The phylogenetic analysis of the DNA sequences led to the  
 922 identification of four clades. The branch lengths represent the percentage of  
 923 phylogenetic distance. (B) The *Rpi-chc1* alleles belong to the CNL immune receptor  
 924 family. Different motifs were found in the different receptor domains. The LRR  
 925 domain consists of 29 imperfect repeats.  
 926

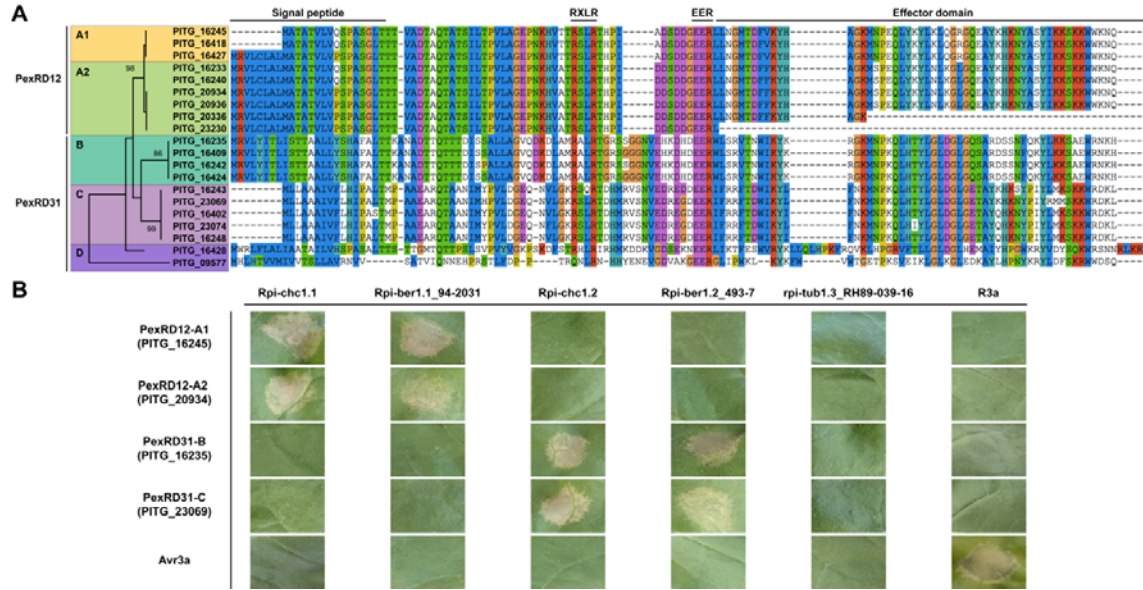
927



928

929 **Fig. 3.** The RXLR effector PexRD12 corresponds to Avrchc1.1.  
930 (A) The three *Rpi-chc1.1* candidates were co-infiltrated with the Pex effector  
931 collection in *N. benthamiana* leaves to screen for Avrchc1.1. *Rpi-chc1.1* induces cell  
932 death when co-expressed with both PITG\_16233 and PITG\_16240, from the  
933 PexRD12 family. *R3a* and *Avr3a* were used as negative controls, a mix of *R3a* and  
934 *Avr3a* were used as a positive control. (B) Relative *Avrchc1.1* and *Avrsto1*  
935 effector expression in *P. infestans* field isolates collected from untransformed Desiree plants,  
936 and Desiree plants transformed with *Rpi-chc1* (Desiree:*Rpi-chc1.1*), or *Rpi-sto1*  
937 (Desiree:*Rpi-sto1*) (2013, Wageningen). Three independent samples were included  
938 in the RT-qPCR experiment. Stars represent statistical difference in a two sample T-  
939 test,  $p < 0.008$ .  
940

941



942

943

**Fig. 4.** Rpi-chc1 alleles show non-overlapping recognition of the PexRD12/31 effector superfamily.

944

(A) The twenty members of the PexRD12/31 superfamily found in *P. infestans* isolate T30-4. In the amino acid sequence we can distinguish a signal peptide in the N-terminus, the conserved RXLR-EER motifs in the center, and the effector domain in the C-terminus. Some PexRD12/31 family members differed at the nucleotide level but were identical at the protein level (PITG\_16245 = PITG\_16418; PITG\_16233 = PITG\_16240; PITG\_20934 = PITG\_20936; PITG\_16409 = PITG\_16424). The phylogenetic analysis of the complete protein sequences led to the identification of five clades. This analysis was performed in MEGA X by using the Maximum Likelihood method based on the JTT matrix-based model. The tree with the highest log likelihood (-766) is shown. The bootstrapping values, which indicates the percentage of trees that had the particular branch, are shown in each branch. (B) Different *Rpi-chc1* allelic variants were co-agroinfiltrated in *N. benthamiana* with a member from each PexRD12/31 clade. While variants from clade 1 recognize both PexRD12 A1 and A2 clades, *Rpi-chc1* variants from clade 2 recognize PexRD31 B and C. A mix of *R3a* and *Avr3a* was used as a positive control.

945

946

947

948

949

950

951

952

953

954

955

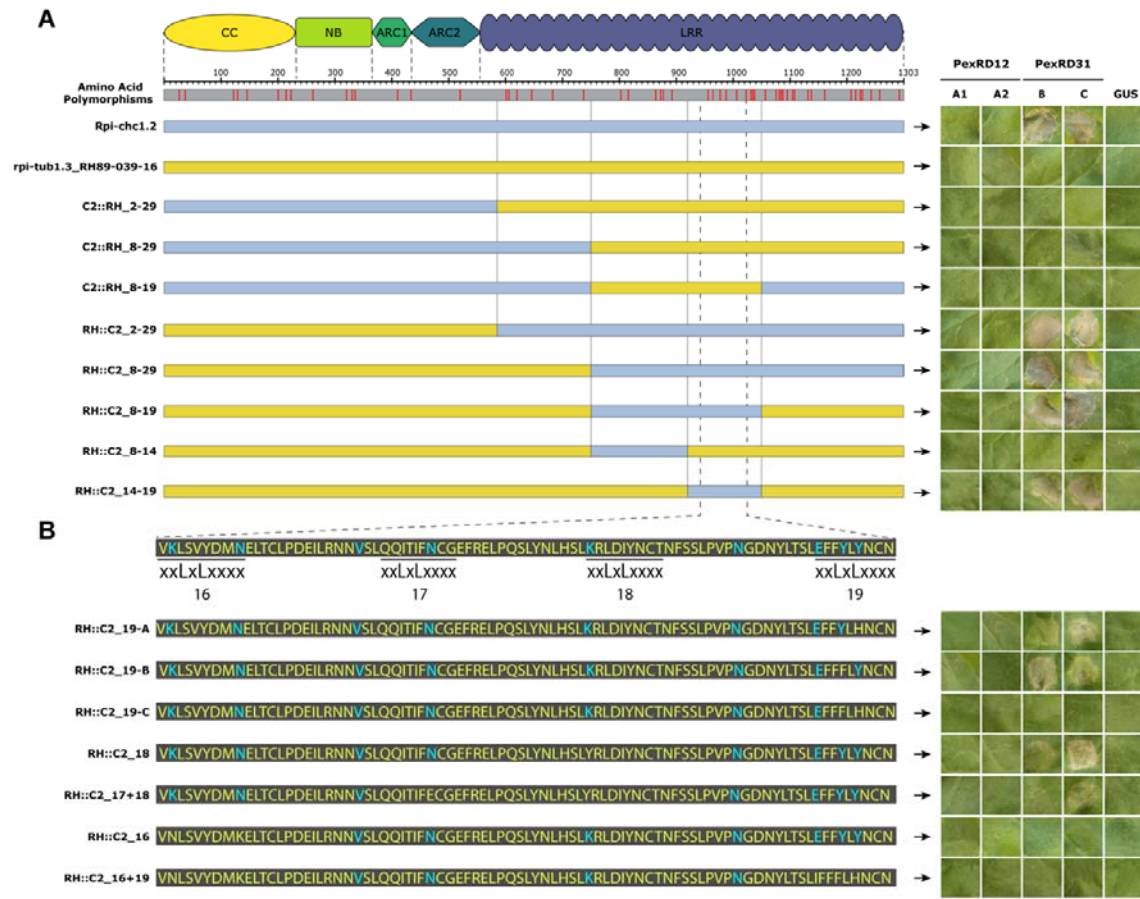
956

957

958

959

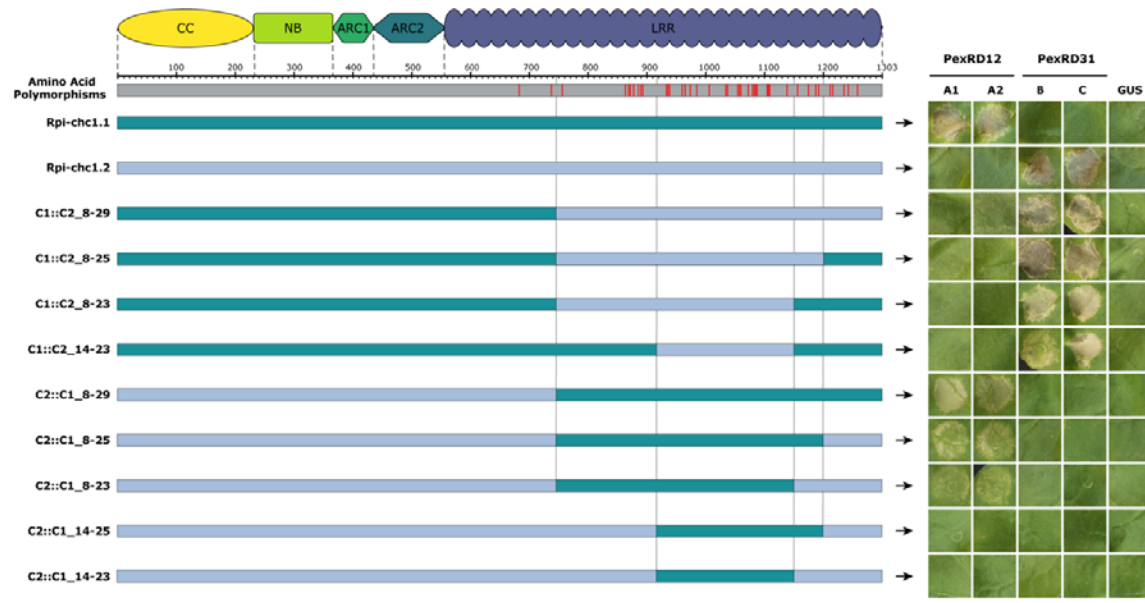
960



961  
962  
963  
964  
965  
966  
967  
968  
969  
970  
971  
972  
973  
974  
975  
976  
977  
978  
979  
980  
981  
982  
983

**Fig. 5.** Domain exchanges between rpi-tub1.3\_RH89-039-16 and Rpi-chc1.2. (A) The positions of SAPs and the corresponding protein domains are indicated on top. Rpi-chc1.2 and rpi-tub1.3\_RH89-039-16, are represented as light blue and yellow bars, respectively. Below, the domain exchanges are shown. The chimeric constructs were co-agroinfiltrated with the PexRD12/31 effectors in *N. benthamiana* leaves. After 4 days, the HR that was visible and recorded. Experiments were repeated three times with 12 inoculation sites each time. A representative leaf for the response of each chimeric construct is shown in the right panel. GUS was used as a negative control. It is concluded that the exchange of the complete LRR domain led to recognition of PexRD31. With the final construct, RH::C2\_14-19, the exchange of only nine amino acids led to the activation of the rpi-tub1.3\_RH89-036-16 protein. (B) Pinpointing of the amino acids involved in the Rpi-chc1.2 recognition specificity. SAPs are highlighted in blue font. Most of the SAPs are located in the solvent exposed xxLxLxxxx motif of the LRR 16-19. The chimeric constructs were co-agroinfiltrated with the PexRD12/31 effectors in *N. benthamiana* leaves. A representative leaf for the response of each chimeric construct is shown in the right panel. Experiments were repeated three times with 12 inoculation sites each time. GUS was used as a negative control. The modification of any of the Rpi-chc1.2 solvent exposed specific amino acids (blue) for the corresponding amino acid present in rpi-tub1.3\_RH89-039-16 (yellow), led to the partial or complete loss of effector recognition.

984



985

986

987

988

989

990

991

992

993

994

995

996

997

998

**Fig. 6.** The effector recognition specificity could be exchanged between Rpi-chc1.1 and Rpi-chc1.2.

The alignment of Rpi-chc1.1 and Rpi-chc1.2 shows that all the 41 amino acids polymorphisms (red bars) are located in the LRR domain. The chimeric constructs were co-agroinfiltrated with the PexRD12/31 effectors in *N. benthamiana* leaves. A representative leaf for the response of each chimeric construct is shown in the right panel. Experiments were repeated three times with 12 inoculation sites each time. GUS was used as a negative control. In the construct C1::C2\_14-23, we could see that the LRR 16-19 reappear again as determining for the PexRD31 recognition. The required domain exchanges of the Rpi-chc1.1 LRR are more complex and encompasses almost the complete LRR.



999 **Supporting Information:**

1000

1001 Fig. S1: pBINPLUS-PASSA-GG vector map.

1002 Fig. S2: Inoculation of *P. infestans* on *N. benthamiana* leaves agroinfiltrated with *Rpi-chc1.1*

1003 candidates.

1004 Fig. S3: Effector and R gene expression in potato leaves inoculated with *P. infestans*.

1005 Fig. S4: Rpi-chc1.1 protein domain organization.

1006 Fig. S5: Localization of PexRD12/31 effectors in the *P. infestans* T30-4 contigs.

1007 Table S1: Accession numbers of Solanum genotypes and Rpi-chc1 sequences

1008 Table S2: Primers used in this study.

1009 Table S3: *P. infestans* effectors used in this study.

1010 Table S4: CRISPR-Cas9 targeting of Rpi-chc1.1.

1011 Table S5: Late blight resistance assessment of different Rpi-chc1 alleles.

1012 Table S6: Segregation of markers and late blight resistance of Rpi-chc1.1 and Rpi-chc1.2.

1013 Table S7: Functional expression of Rpi-chc1.1 in Desiree transgenic events correlates with

1014 responsiveness to PexRD12.